

## Effect of Al and N Doping on Structural and Optical Properties of Sol-Gel Derived ZnO Thin Films

(Kesan Pendedopan Al dan N Terhadap Struktur dan Sifat Optik Filem Nipis  
ZnO yang disediakan Melalui Kaedah Sol-Gel)

CHATPONG BANGBAI\*, KRISANA CHONGSRI, WISANU PECHARAPA & WICHARN TECHITDHEERA

### ABSTRACT

*In this work, the preparation of ZnO, N-doped ZnO (NZO), Al-doped ZnO (AZO) and Al, N-doped ZnO (ANZO) thin films by the sol-gel spin-coating method is reported. The structural properties and surface morphologies of films were characterized by X-ray diffraction (XRD) and field emission scanning electron microscope (FE-SEM). The optical properties of the films were interpreted from their transmission spectra using UV-VIS spectrophotometer. The XRD and SEM results disclosed that the crystallization quality and grain size of as-prepared films were highly influenced by N and Al doping. UV-VIS spectrophotometer results indicated that Al and N additives could significantly enhance the optical transparency and induce the blue-shift in optical bandgap of ZnO films.*

*Keywords:* Al doping; N doping; sol-gel; ZnO thin films

### ABSTRAK

*Di dalam kajian ini, penyediaan saput tipis ZnO, N-terdop ZnO (NZO), Al-terdop ZnO (AZO) dan Al, N-terdop ZnO (ANZO) menggunakan kaedah salutan-putaran sol-gel dilaporkan. Sifat-sifat struktur dan morfologi permukaan filem dicirikan menggunakan pembelauan sinar-X (XRD) dan mikroskop imbasan elektron pancaran medan (FE-SEM). Sifat optik filem tersebut diperoleh daripada spektrum transmisi dengan menggunakan spektrofotometer UV-VIS. Keputusan XRD dan SEM membuktikan bahawa kualiti penghabluran dan saiz butiran filem yang disediakan sangat dipengaruhi oleh pendopan N dan Al. Keputusan UV-VIS spektrofotometer menunjukkan bahawa bahan tambahan Al dan N dapat meningkatkan kelutsinaran optik dan mempengaruhi anjakan-biru antara jurang jalur optik filem ZnO secara signifikan.*

*Kata kunci:* Pendedopan Al; pengedopan N; saput tipis ZnO; sol-gel

### INTRODUCTION

With a wide bandgap of 3.37 eV and high exciton binding energy of 60 meV at room temperature (Zeng et al. 2007), zinc oxide (ZnO) is one of most widely used materials for ultraviolet optoelectronic devices such as light emitting diodes (LED) (Chichibu et al. 2005), laser diodes (Znaidia et al. 2003) and ultraviolet photodetectors (Zhou et al. 2011). Up to now, ZnO films have been fabricated by various physical and chemical techniques, which include RF magnetron sputtering (Zhang et al. 2006), pulsed laser deposition (Cracium et al. 1994), chemical vapor deposition (Kashiwaba et al. 2002), spray pyrolysis (Ayouchi et al. 2003) and sol-gel processing (Kim & Tai 2007). The sol-gel route process has significant advantages over the other deposition techniques due to low-cost experimental arrangement, ease of adding dopant, high homogeneity, excellent compositional control, lower crystallization temperature and relatively low process temperature.

A number of reports have recently dedicated on the effort to adjust the properties of ZnO by doping with group V elements such as As, P and N. Generally, the light doping of impurities such as Al, In, B, Ga into

ZnO causes the drastic change in electrical conductivity (Nunes et al. 2002). Meanwhile, nitrogen is known as a preferable dopant due to its considerable advantages such as low toxicity, low ionization energy and source abundance. Nitrogen has been utilized as an effective dopant to adjust the optical or electrical properties variety of semiconductors including ZnO (Wang et al. 2011). Zou et al. (2009) prepared ZnO:N films on glass substrates by thermal oxidation of  $Zn_3N_2$  precursor and reported that the doped films exhibited p-type semiconductor behavior with strongly temperature-dependent conductivity. Sui et al. (2010) employed radio-frequency magnetron sputtering technique to grow B-N codoped ZnO (ZnO:(B,N)) films and they observed that this co-doping was able to generate the p-type manner and the post-annealing had significant effects on not only electrical conductivity but optical properties of the films. Xue et al. (2006) gave the report on the preparation of ZnO:Al films by sol-gel method and it was found that Al-doping concentration played a major role on the enhancement of transparency and the shift of optical bandgap of ZnO thin films. Nevertheless, up to now, reports on the preparation and characterization of

Al-N codoped ZnO films by sol-gel method are still very limited.

The main propose of this paper was concentrated on the preparation of Al and N-doped ZnO (ANZO) thin films by sol-gel spin coating technique. The effects of Al and N doping on the structural and optical properties of the films were extensively investigated.

#### MATERIALS AND METHODS

The precursor sol was prepared from zinc acetate dehydrate ( $(\text{CH}_3\text{COO})_2\text{Zn}\cdot 2\text{H}_2\text{O}$ ), absolute ethanol ( $\text{C}_2\text{H}_5\text{OH}$ ) and diethanolamine ( $(\text{HOCH}_2\text{CH}_2)_2\text{NH}$ , DEA). Aluminium acetate ( $\text{C}_4\text{H}_7\text{AlO}_3$ ) and ammonium acetate ( $\text{CH}_3\text{COONH}_4$ ) were introduced as dopants. The prepared mixture was vigorously stirred at  $100^\circ\text{C}$  for 6 h by magnetic stirrer and cooled to room temperature for 24 h. The Al and N doping contents in ZnO were 5 at.% and 10 at.%. Al-N codoped ZnO (ANZO) samples with the Zn:Al:N concentration ratio of 0.90:0.05:0.05, 0.85:0.05:0.10, 0.85:0.10:0.05 and 0.80:0.10:0.10 are designated as ANZO1, ANZO2, ANZO3 and ANZO4, respectively. All films were spin-coated on borosilicate substrates at room temperature with speed of 2,500 rpm for 20 s followed by pre-heated in air at  $100^\circ\text{C}$  for 10 min. After repeating the coating procedure three times, all films were annealed at  $550^\circ\text{C}$  for 4 h in ambient air. The structural properties and surface morphologies of as-prepared films were characterized by X-ray diffraction (XRD, Panalytical x'Pert Pro MPD) using  $\text{Cu-K}_\alpha$  radiation over a  $2\theta$  in the range of  $20$ - $60^\circ$ . The diffraction patterns were recorded with a scanning rate  $2^\circ/\text{min}$ . The surface morphology and film thickness were examined by field emission-scanning electron microscope (FE-SEM, Hitachi S-4700) operated at 10 kV after coating with gold. The chemical compositions of the films were examined by an energy dispersive X-ray spectrometer (EDS). The

optical properties of the films were interpreted from their transmission spectra using UV-VIS spectrophotometer (Thermo Electron Corporation Helios $\alpha$ ).

#### RESULTS AND DISCUSSION

The XRD patterns of NZO thin films with various doping content of 0%, 5 at.% and 10 at.% are illustrated in Figure 1(a). The distinct diffraction peaks located at  $2\theta=31.8^\circ$ ,  $34.5^\circ$ ,  $36.2^\circ$ ,  $47.5^\circ$  and  $56.7^\circ$  are assigned to (100), (002), (101), (102) and (110) orientation planes of ZnO with hexagonal wurtzite structure, respectively (Zhang 2010). As observed in XRD patterns, both pure and N-doped films possess three strong diffracted peaks advising that as-prepared films have single-phase polycrystalline structure without any preferable orientation. This manner of XRD patterns is typically a formation of sol-gel derived ZnO (Wang et al. 2006). Average grain sizes of all films can be calculated from the full width at half maximum (FWHM) and angular position of three distinct diffraction peaks by well-known Scherrer's formula. The average grain sizes of undoped and N-doped ZnO films expressed in Figure 1(b) are found to be in the range of 38-40 nm, changing upon doping content. The results indicated that the crystallite size of the film slightly increases as the N doping content increases up to 5 at.% thereafter decreases. The increase of grain size of sol-gel derived ZnO films with certain N-doping content may originate from the formation of intermediate buffer layer of Zn and N that can improve the crystallization of the film (Liu et al. 2010). The XRD patterns of AZO with various Al doping content of 0%, 5 at.% and 10 at.% is illustrated in Figure 2. In the same manner, the position of three characteristic peaks of (100), (002) and (101) orientation planes still remain the same position as Al doping content varies, indicating stability of hexagonal crystalline structure of ZnO films deposited

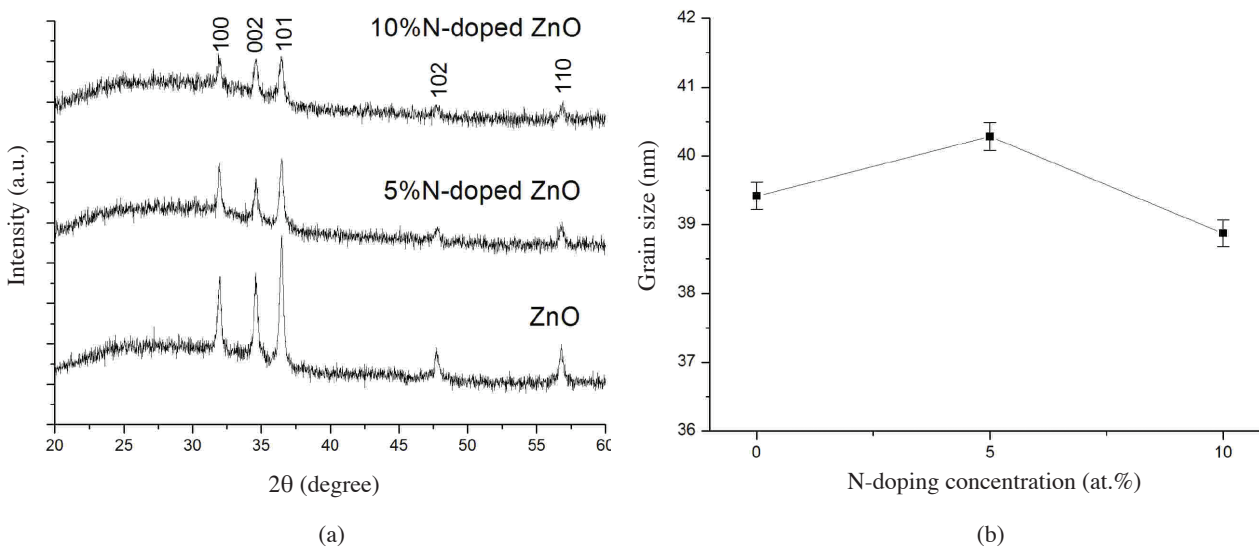


FIGURE 1. (a) XRD patterns of sol-gel spin-coated N-doped ZnO thin films with different N doping concentrations and (b) the calculated grain size of N-doped ZnO films with different N doping concentrations

on glass substrates. Besides, significant deterioration in crystallinity of the films was observed in Al-doped films, accompanying the decreasing intensities and the widening of XRD peaks with the increase of Al content. This feature is in good agreement with prior report (Zi-qiang et al. 2006). Based on Scherrer's equation, it is suggested that the decrease of average grain size of ZnO films is strongly affected by Al doping. As seen in XRD patterns of AZO films, no characteristic peak of crystalline  $\text{Al}_2\text{O}_3$  is observed because of the rather high enthalpy required (Kou et al. 2006). At annealing temperature, aluminium atom doped into the films may form amorphous  $\text{Al}_2\text{O}_3$  and deter the grain growth of ZnO films (Wang et al.

2009), reflecting the deterioration of grain size of doped films. XRD patterns of AZNO films are shown in Figure 3. All codoped films exhibited unobvious XRD patterns of ZnO, suggesting that the codoping of Al and N strongly affects the decrystallization of ZnO films leading to higher degree of amorphousity of ZnO with increasing doping content. Due to the different ionic radius between  $\text{Al}^{3+}$  (53 pm) and  $\text{Zn}^{2+}$  (72 pm) (Kim et al. 1997) and between N (171 nm) and O (140 nm) (Zhao et al. 2012), the substitutional replacement of Al at Zn site and N at O site may generate the local stresses that takes a major contribution on the prevention of crystal growth of ZnO (Zi-qiang et al. 2006).

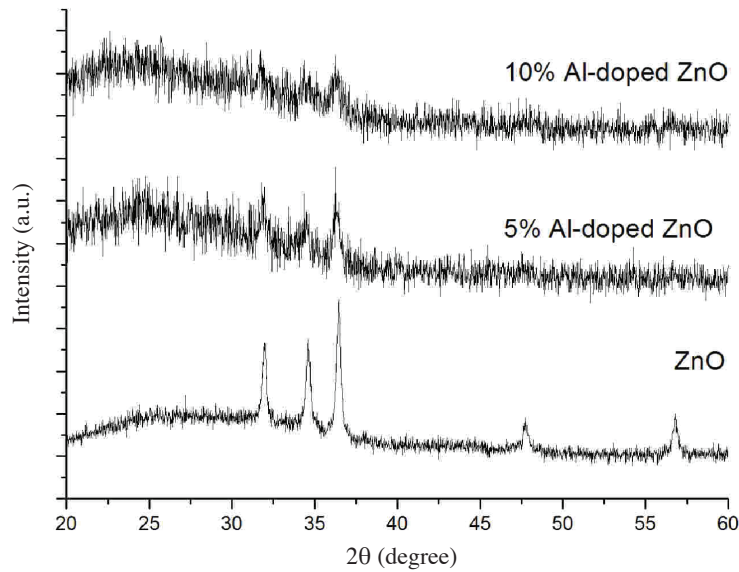


FIGURE 2. XRD patterns of sol-gel spin-coated AZO thin films with different Al doping concentrations

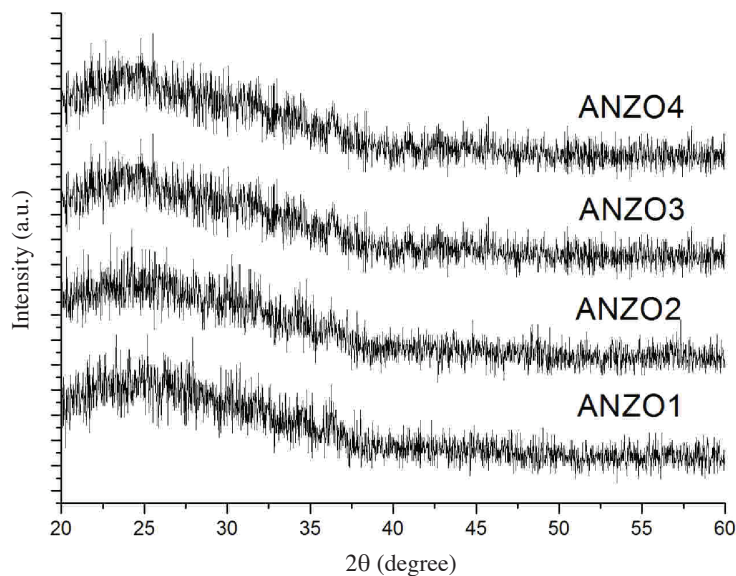


FIGURE 3. XRD patterns of sol-gel spin-coated ANZO thin films with different Al, N doping concentrations

Figure 4(a) shows a cross section image of 5% N-doped ZnO film, indicating the consistence of the film formation on glass substrate with average thickness of approximately 400 nm. The thicknesses of the others were found to be in the same value. Figures 4(b) to 4(d) illustrate surface morphologies of undoped film, 5 at.% N-doped film and 10 at.% N-doped film, respectively. It is clearly observed that all films have smooth surface comprising uniform grain size. It is observable that, when comparing to undoped film, the N-doped films display the amelioration of grain density of the film and the change in grain size. The grain size of the film increases for 5 at.% N concentration and thereafter decreases. The behavior dealing with the decrease in grain size above the specific doping concentration was also supported by other previous

literature (Bouzidi et al. 2010). The SEM results are in good agreement to results interpreted from XRD patterns. The chemical composition of 5 at.% N-doped film and 10 at.% N-doped film indicated by EDS spectra are shown in Figures 4(e) and 4(f), respectively. The atomic percentage of N doping in the films exhibit close agreeable to the ratio of the precursors in the solution for coating. Figure 5(a) exhibits the cross section image of 5 at.% Al-doped film indicating the uniform thickness of about 400 nm. Meanwhile, Figures 5(b) to 5(d) illustrate surface morphologies of undoped film, 5 at.% Al-doped film and 10 at.% Al-doped film, respectively. It is evidently observed that the grain size of the film drastically decreases as Al-doping content increases, which confirms the presumption from the XRD results. With increasing doping content, the crystallite is

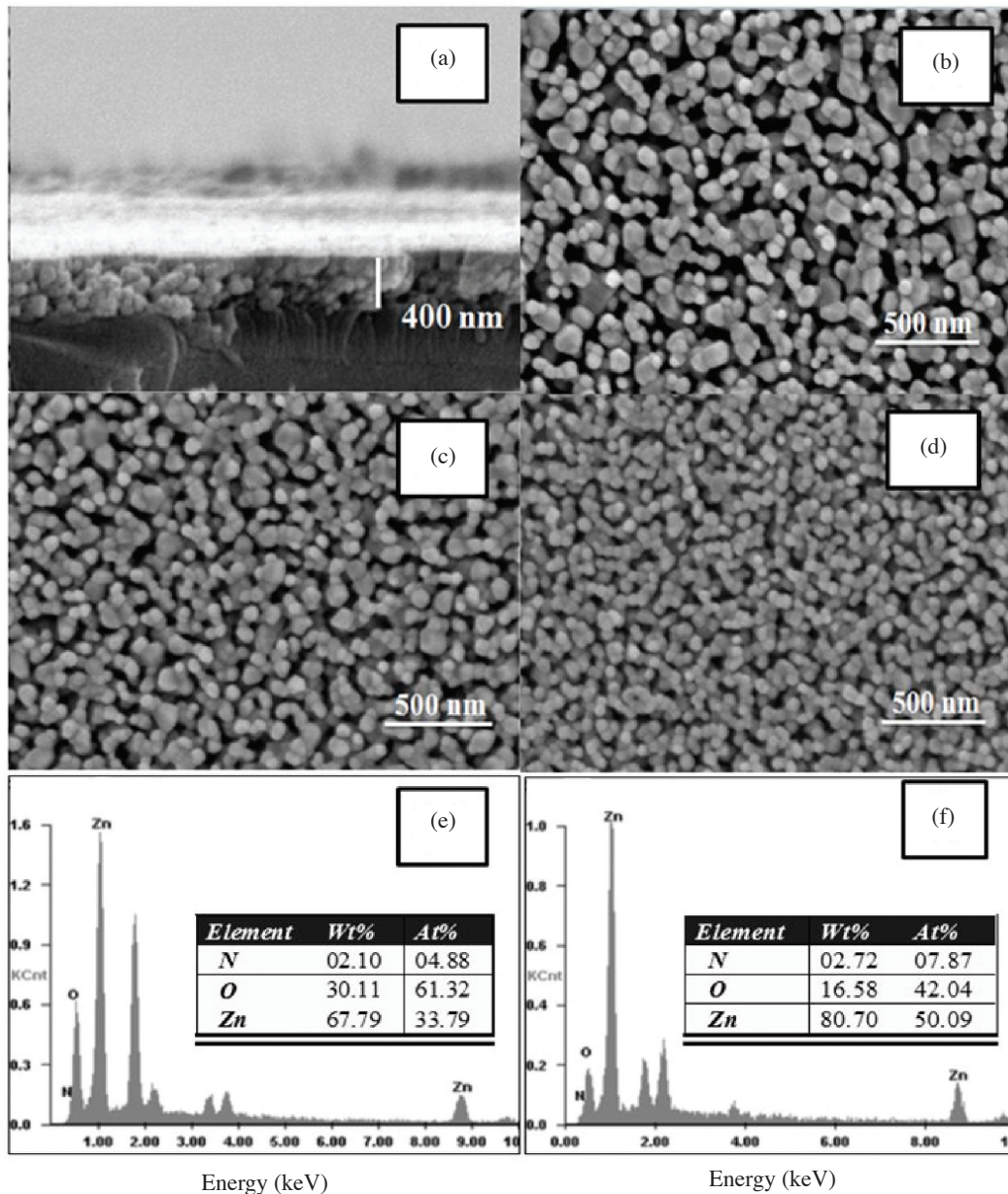


FIGURE 4. (a) cross-section image of 5 at.% N-doped ZnO thin film, SEM images of (b) undoped ZnO, (c) 5 at.% N-doped ZnO, (d) 10 at.% N-doped ZnO thin films and EDS spectrum of (e) 5 at.% N-doped ZnO and (f) 10 at.% N-doped ZnO thin films

unable to further decrease in nanometer regime resulting to the domination of an amorphous phase of the films. In addition, the corresponding EDS spectra of 5 at.% Al-doped film, 10 at.% Al-doped film, confirming the close chemical composition of Al doping to prepared-precursors are represented in Figures 5(e) and 5(f), respectively.

Figure 6 shows the room temperature optical transmission spectra of as-prepared ZnO, NZO, AZO and ANZO thin films in the wavelength range of 300-800 nm. Transmission spectra of as-prepared thin films possess prominent absorption edge in visible range, suggesting good quality of films attained by spin coating technique. Comparing to undoped film, the spectra of doped films display significantly enhanced transmittance in visible wavelength region of 400-800 nm with more than 85-95% transparency. Besides, for NZO films, their transmission spectra exhibit the noticeable blue shift of absorption edge to lower wavelength with increasing N-doping content,

reflecting the widening of optical bandgap of the film. The identical blue shift behavior with increasing doping content is also observed in AZO films. As shown in Figure 7, co-doping with Al and N into ZnO films also leads to the increase of bandgap with certain doping content, thereafter decreases. The lower bandgap in ANZO4 may be due to the over doping Al content causing the ease of formation and segregation of  $\text{Al}_2\text{O}_3$  in the ZnO films. The corresponding optical bandgaps of all thin films were typically calculated by the following equation:

$$ahv = A(hv - E_g)^{1/2}, \quad (1)$$

where  $E_g$  is the optical bandgap energy,  $A$  is a constant having values between  $1 \times 10^5 \text{ cm}^{-1} \text{ eV}^{-1}$  to  $1 \times 10^6 \text{ cm}^{-1} \text{ eV}^{-1}$ ,  $h\nu$  is photon energy and  $\alpha$  is an absorption coefficient. The variation of optical bandgap of all thin films as a function of Al and N doping concentration is summarized in Table

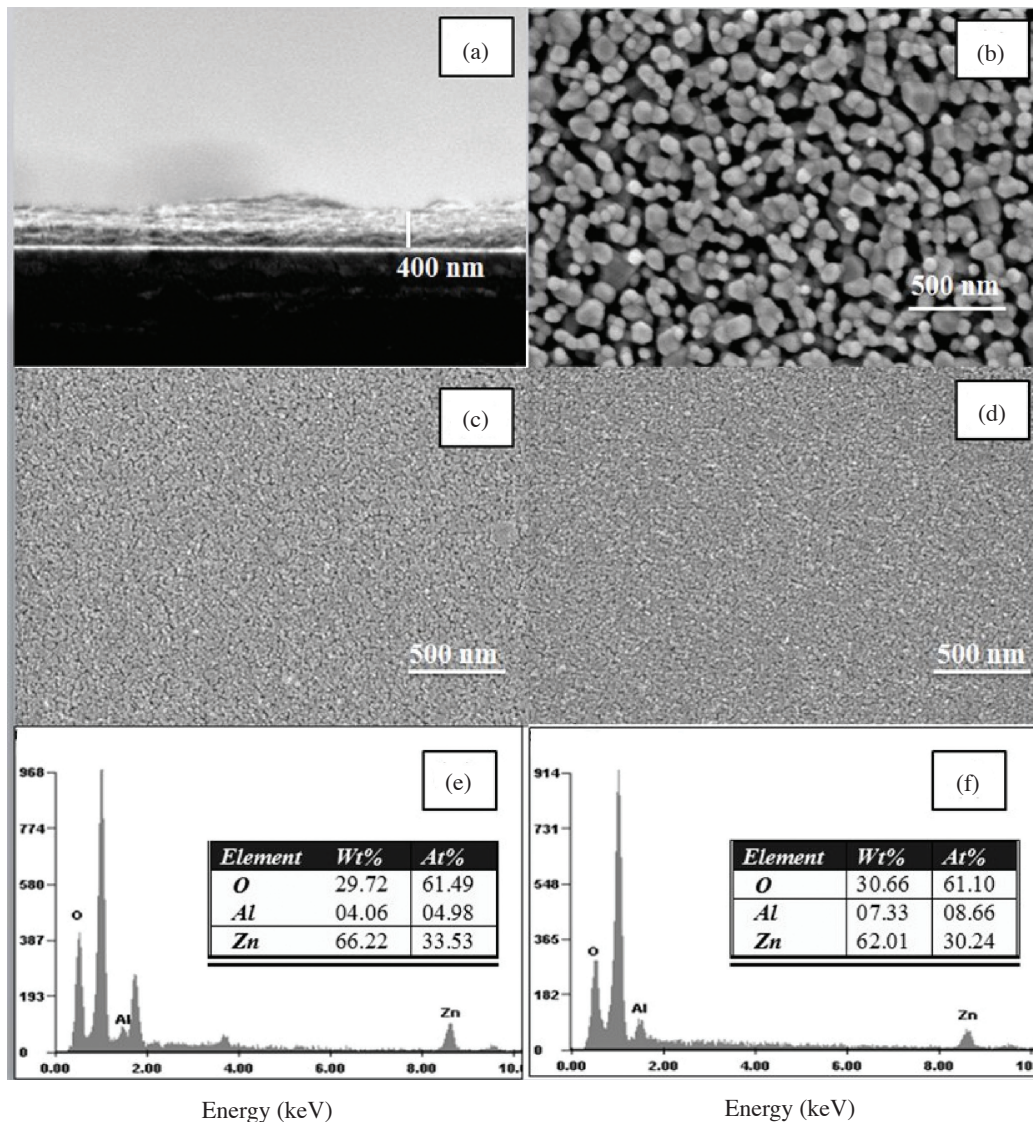


FIGURE 5. (a) cross-section image of 5 at.% Al-doped ZnO thin film, SEM images of (b) undoped ZnO, (b) 5 at.% Al-doped ZnO, (c) 10 at.% Al-doped ZnO thin films and EDS spectrum of (e) 5 at.% Al-doped ZnO and (f) 10 at.% Al-doped ZnO thin films

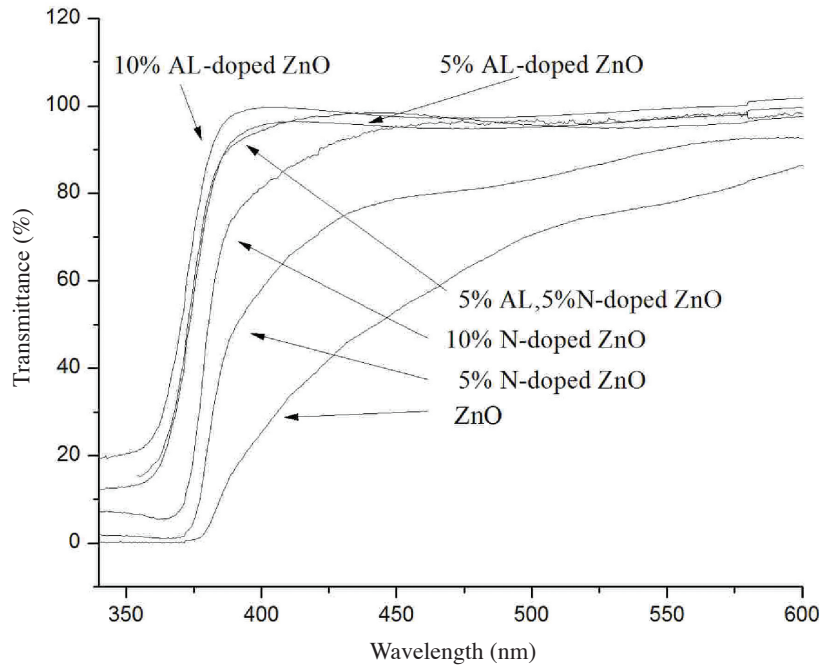


FIGURE 6. Optical transmittance spectra of Al,N-doped ZnO thin films

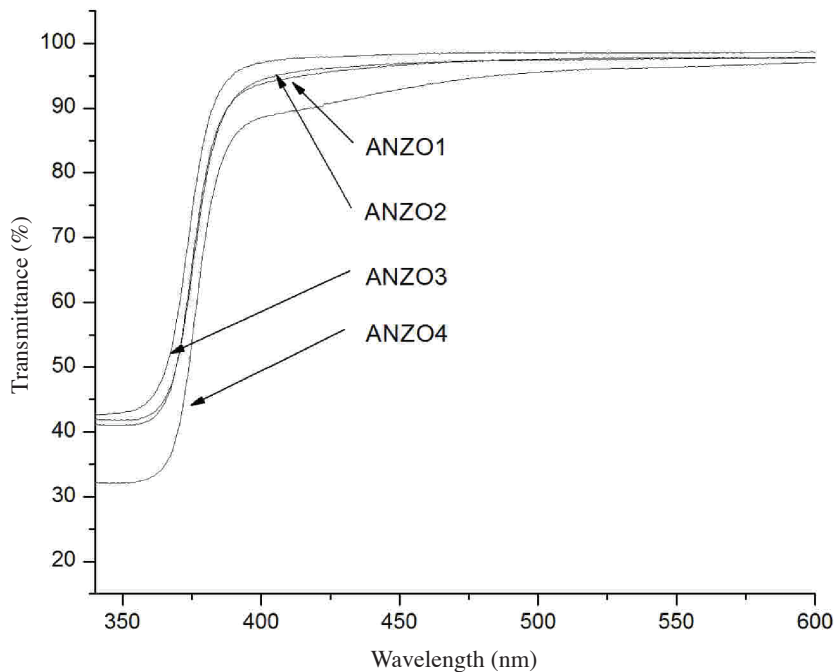


FIGURE 7. Optical transmittance spectra of ANZO thin films

1. From the calculation, the bandgap of the NZO thin films increases from 3.22 to 3.27 eV as the N-doping content increases from 0 at.% to 10 at.%, respectively. Meanwhile, the bandgaps of the AZO thin films slightly increase from 3.22 to 3.25 eV as the Al-doping content increases from 0 at.% to 10 at.%, which is in good agreement to other former published work (Kim & Tai 2007). The feature regarding the increase of optical bandgap with increasing

doping concentration may be attributed to the truth that N or Al dopant may increase the carrier concentration of the film resulting in the carrier-induced widening of bandgap, well-known as Burstein-Moss effect (Li et al. 2010). The other possible mechanism taking responsibility on this widening of the bandgap is the quantum size effect of the nanocrystalline structure of the films (Marotti et al. 2006).

TABLE 1. The calculated optical bandgap of all thin films as a function of Al, N-doping concentration

Al doping concentration (at.%)	N doping concentration (at.%)	Bandgap (eV)
0	0	3.22
0	5	3.26
0	10	3.27
5	0	3.24
5	5	3.23
5	10	3.23
10	0	3.25
10	5	3.27
10	10	3.25

## CONCLUSIONS

ANZO thin films with hexagonal wurtzite type polycrystalline structure and good optical properties have been prepared on glass substrates by sol-gel spin coating and annealing process. The XRD and SEM results disclosed that the crystallization quality and grain size of as-prepared films were highly influenced by both N and Al doping. In addition, the Al and N doping significantly caused the blue shift of the direct bandgap of the films, which were beyond 3.22 eV of pure ZnO and the enhancement of the film transparency in the visible region. These features can be utilized for the feasibility to improve optical performance of ZnO films for ultraviolet optoelectronic devices.

## ACKNOWLEDGEMENTS

This work has been partially supported by the National Nanotechnology Center (NANOTEC), NSTDA and the Ministry of Science and Technology, Thailand, through its program of Center of Excellence Network. This work was funded by the National Electronics and Computer Technology Center (NECTEC). The authors would like to thank Thai Microelectronic (TMEC) for FE-SEM measurement and Rajamangala University of Technology Thanyaburi (RMUTT) for XRD measurement.

## REFERENCES

- Ayouchi, R., Leinen, D., Martin, F., Gabas, M., Dalchiele, E. & Ramos-Barrado, J.R. 2003. Preparation and characterization of transparent ZnO thin films obtained by spray pyrolysis. *Thin Solid Films* 426: 68-77.
- Bouzidi, A., Benramdane, N., Medles, M., Khadraoui, M., Bresson, S., Mathieu, C., Desfeux, R. & Marssi, M. El. 2010. Synthesis of LiVO<sub>3</sub> thin films by spray pyrolysis technique. *Journal of Alloys and Compounds* 503(2): 445-448.
- Chichibu, S.F., Ohmori, T., Shibata, N., Koyama, T. & Onuma, T. 2005. Fabrication of p-CuGaS<sub>2</sub>/n-ZnO: Al heterojunction light-emitting diode grown by metalorganic vapor phase epitaxy and helicon-wave-excited-plasma sputtering methods. *Journal of Physics and Chemistry of Solids* 66: 1868-1871.
- Cracium, V., Elders, J., Gardeniers, J.G.E. & Boyd, I.W. 1994. Characteristics of high quality ZnO thin films deposited by pulsed laser deposition. *Applied Physics Letters* 65(23): 2963-2965.
- Kashiwaba, Y., Sugawara, K., Haga, K., Watanabe, H., Zhang, B.P. & Segawa, Y. 2002. Characteristics of c-axis oriented large grain ZnO films prepared by low pressure MO-CVD method. *Thin Solid Films* 411: 87-90.
- Kim, K.H., Park, K.C. & Ma, D.Y. 1997. Structural, electrical and optical properties of aluminum doped zinc oxide films prepared by radio frequency magnetron sputtering. *Journal of Applied Physics* 81: 7764-7772.
- Kim, Y.S. & Tai, W.P. 2007. Electrical and optical properties of Al-doped ZnO thin films by sol-gel process. *Applied Surface Science* 253: 4911-4916.
- Kuo, S.Y., Chen, W.C., Lai, F.I., Cheng, C.P., Kuo, H.C., Wang, S.C. & Hsieh, W.F. 2006. Effects of doping concentration and annealing temperature on properties of highly-oriented Al-doped ZnO films. *Journal of Crystal Growth* 287(1): 78-84.
- Li, C., Meng, F.Y., Zhang, S. & Wang, J.Q. 2010. Effects of Mg content and B doping on structural, electrical and optical properties of Zn<sub>1-x</sub>Mg<sub>x</sub>O thin films prepared by MOCVD. *Journal of Crystal Growth* 312: 1929-1934.
- Liu, W.W., Yao, B., Li, Y.F., Li, B.H., Zhang, Z.Z., Shan, C.X., Zhang, J.Y., Shen, D.Z. & Fan, X.W. 2010. P-Type MgZnO thin films grown using N delta-doping by plasma-assisted molecular beam epitaxy. *Journal of Alloys and Compounds* 504: 484-487.
- Marotti, R.E., Giorgi, P., Machado, G. & Dalchiele, E.A. 2006. Crystallite size dependence of band gap energy for electrodeposited ZnO grown at different temperatures. *Solar Energy Materials and Solar Cells* 90: 2356-2361.
- Nunes, P., Fortunato, E., Tonello, P., Fernandes, F.B., Vilarinho, P. & Martins, R. 2002. Effect of different dopant elements on the properties of ZnO thin films. *Vacuum* 64: 281-285.
- Sui, Y.R., Yao, B., Yang, J.H., Gao, L.L., Yang, T., Deng, R., Ding, M., Zhao, T.T., Huang, X.M., Pan, H.L. & Shen, D.Z. 2010. Post-annealing influence on electrical properties and photoluminescence of B-N codoping ZnO thin films. *Journal of Luminescence* 130: 1101-1105.

- Wang, J., Meng, L., Qi, Y., Li, M., Shi, G. & Liu, M. 2009. The Al-doping contents dependence of the crystal growth and energy band structure in Al:ZnO thin films. *Journal of Crystal Growth* 311: 2305-2308.
- Wang, M., Wang, J., Chen, W., Cui, Y. & Wang, L. 2006. Effect of preheating and annealing temperatures on quality characteristics of ZnO thin film prepared by sol-gel method. *Materials Chemistry and Physics* 97: 219-225.
- Wang, T., Liu, Y., Fang, Q., Wu, M., Sun, X. & Lu, F. 2011. Low temperature synthesis wide optical band gap Al and (Al, Na) co-doped ZnO thin films. *Applied Surface Science* 257: 2341-2345.
- Xue, S.W., Zu, X.T., Zheng, W.G., Chen, M.Y. & Xiang, X. 2006. Effects of annealing and dopant concentration on the optical characteristics of ZnO:Al thin films by sol-gel technique. *Physica B* 382: 201-204.
- Zeng, Y.J., Ye, Z.Z., Xu, W.Z., Liu, B., Che, Y., Zhu, L.P. & Zhao, B.H. 2007. Study on the Hall-effect and photoluminescence of N-doped p-type ZnO thin films. *Materials Letters* 61: 41-44.
- Zhang, C. 2010. High-quality oriented ZnO films grown by sol-gel process assisted with ZnO seed layer. *Journal of Physics and Chemistry of Solids* 71: 364-369.
- Zhang, Z., Zhang, Y., Duan, L., Lin, B. & Fu, Z. 2006. Deep ultraviolet emission of ZnO films prepared by RF-magnetron sputtering at changing substrate temperature. *Journal of Crystal Growth* 290: 341-344.
- Zhao, Y., Peng, X., Li, Z., Zhou, M., Liang, X., Wang, J., Min, J., Wang, L. & Shi, W. 2012. The photoluminescence characterization of the N-doped ZnO films produced by wet chemical deposition. *Applied Physics A* 107: 959-963.
- Zhou, H., Fang, G.J., Liu, N. & Zhao, X.Z. 2011. Effects of thermal annealing on the performance of Al/ZnO nanorods/Pt structure ultraviolet photodetector. *Materials Science and Engineering B* 176: 740-744.
- Zi-qiang, X., Hong, D., Yan, L. & Hang, C. 2006. Al-doping effects on structure, electrical and optical properties of c-axis-orientated ZnO: Al thin films. *Materials Science in Semiconductor Processing* 9: 132-135.
- Znaidia, L., Soler Illia, G.J.A.A., Benyahia, S., Sanchez, C. & Kanaev, A.V. 2003. Oriented ZnO thin films synthesized by sol-gel process for laser application. *Thin Solid Films* 428: 257-262.
- Zou, C.W., Chen, R.Q. & Gao, W. 2009. The microstructures and the electrical and optical properties of ZnO: N films prepared by thermal oxidation of Zn<sub>3</sub>N<sub>2</sub> precursor. *Solid State Communications* 149: 2085-2089.

Chatpong Bangbai\* & Wicharn Techitdheera  
School of Applied Physics  
King Mongkut's Institute of Technology Ladkrabang  
Ladkrabang, Bangkok, 10520  
Thailand

Krisana Chongsri  
Department of Applied Physics  
Faculty of Science and Technology  
Rajabhat Rajanagarindra University  
Chachoengsao, 24000  
Thailand

Wisanu Pecharapa  
College of Nanotechnology  
King Mongkut's Institute of Technology Ladkrabang  
Ladkrabang, Bangkok 10520  
Thailand

Wisanu Pecharapa  
ThEP Center  
CHE, 328 Siayuthtaya Rd.  
Bangkok, 10400  
Thailand

\*Corresponding author; email: chatpong\_b@windowslive.com

Received: 7 January 2012

Accepted: 21 May 2012